Conformation of Human Fibrinogen in Solution from Polarized Triplet Spectroscopy†

J. M. Montejo,‡ K. Razi Naqvi,§ M. Pilar Lillo,‡ J. González-Rodríguez,‡ and A. Ulises Acuña*,‡

Instituto de Química Física, CSIC, Serrano 119, 28006 Madrid, Spain, and Department of Physics, University of Trondheim, N-7055 Dragvoll, Norway

Received January 30, 1992; Revised Manuscript Received May 13, 1992

ABSTRACT: The rotational motions of human fibrinogen in solution at 20 °C have been examined, in the 0.2–12-μs time range, by measuring the laser-induced dichroism of the triplet state of an erythrosin probe covalently bonded to the protein. The decay of the anisotropy was multiexponential, and up to three correlation times (ϕ_1 = 380 ± 50 ns, ϕ_2 = 1.1 ± 0.1 μs, and ϕ_3 = 3.3 ± 0.6 μs) were needed to obtain a satisfactory analysis. The experimental data are consistent with the brownian motions of an elongated, rigid particle. If the correlation times are combined with previous data on the intrinsic viscosity of fibrinogen, the rotational and translational diffusive properties of the protein can be reproduced with high accuracy by idealizing it as an elongated ellipsoid of revolution with dimensions ($2a \times 2b$) of (54 ± 6) × (7.2 ± 0.5) nm, having rotational diffusion constants of $D_{\parallel} = (6.2 \pm 0.7) \times 10^5\ s^{-1}$ and $D_{\perp} = (5 \pm 1) \times 10^4\ s^{-1}$. The possibility of Ca^{2+}-dependent changes in the rigidity or conformation of fibrinogen was excluded by examining the submicrosecond time-resolved fluorescence depolarization of 1-methylpyrene conjugates of the protein in the presence of different calcium concentrations. Although there are inherent difficulties to extrapolate the data on isolated fibrinogen molecules to the polymerizing species, this relatively stiff conformation meets the requirements of the classical half-staggered double-stranded model of fibrin polymerization rather better than those of the recently proposed interlocked single-stranded mechanism.

Fibrinogen (340 kDa), a blood plasma multidomain protein (Doolittle, 1973), in addition to being the precursor of fibrin formation plays a second crucial role in hemostasis, by causing platelet agreggation through its binding to a specific receptor at the surface of activated platelets (Kieffer & Philips, 1990; Rivas et al., 1991). Since some aspects of the former process are not fully understood (Hunziker et al., 1990) and most of the second are poorly grasped at a molecular level (Kieffer & Philips, 1990), a precise knowledge of the conformation of fibrinogen in physiological conditions would facilitate the formulation of plausible reaction mechanisms. Accordingly, the size, shape, and possible flexibility of this protein have been scrutinized by a wide array of physicochemical techniques (Doolittle, 1973; Haverkate et al., 1983) ranging from those like electron microscopy (EM), which provides information on the unsolvated molecule, to hydrodynamic and optical–spectroscopic studies, which examine macromolecules in solution. As regards the overall dimensions of the *dry* molecule and its appearance in electron micrographs (Fowler & Erickson, 1979; Erickson & Fowler, 1983; Beijbom et al., 1988), the doubts about the trinodular rod (with dimensions of length 47 ± 2 nm and an average width of 7 ± 2 nm) proposed first by Hall and Slayter (1959) have been dispelled. In contrast, the solution studies have not led to a consensus on the conformation of fibrinogen, and data obtained from small-angle X-ray, neutron, and laser light scattering, ultracentrifugation, viscosimetry, flow birefringence, etc. have been interpreted with disparate geometries that span from disks to very elongated rods [see Doolittle (1973), Bachmann et al. (1975), Lederer (1975), Lederer and Hammel (1975), and López et al. (1984) for reviews]. It should be noted that images of the protein in solution and adsorbed on silicon dioxide surfaces, generated by atomic force microscopy (AFM)[1] (Drake et al., 1989; Wigren et al., 1991), also display the trinodular structure.

We recently presented (Acuña et al., 1987a,b) a time-resolved fluorescence anisotropy study of 1-methylpyrene conjugates of fibrinogen (MePy-FIB) in aqueous, calcium-free solution. This work was aimed at ascertaining the putative flexibility rather than the overall hydrodynamics of the protein, because the microsecond rotation of fibrinogen produces only a very small depolarization of the fluorescence. Nevertheless, an approximate model was proposed there as a rigid (in the 10–1000-ns time window) prolate ellipsoid having dimensions not very different from those observed in the Hall and Slayter EM images. Although this model of fibrinogen was compatible with the reported solution data (Haverkate et al., 1983; Lederer, 1975), much of this hydrodynamic evidence is ultimately based on measurements of the *translational* (D_t) or the *average rotational* diffusion coefficient, neither of which is particularly useful in determining unambiguously a molecular shape. Due to the dearth of more accurate data, alternative shapes of the protein in solution are still being proposed as, e.g., a discoid, assumed to originate from a folded fibrinogen molecule (Larsson et al., 1987).

It has been pointed out (Mueller & Burchard, 1978) that the discordant interpretations of the solution studies might be resolved if fibrinogen had a highly flexible structure; in fact, conformational flexibility around the central domain is frequently invoked (Beijbom et al., 1988) to explain the small

† Supported by grants from the Consejo Superior de Investigaciones Científicas (CSIC-635/070) and the Comisión Interministerial de Ciencia y Technología (CICYT-PB90-0102) and by a NATO Collaborative Research Grant (86/0531). J.M.M. was the recipient of a predoctoral fellowship from the PFPI (Spain).

* To whom correspondence should be addressed.

‡ CSIC.

§ University of Trondheim.

[1] Abbreviations: AFM, atomic force microscopy; FIB, human fibrinogen; MePy, 1-methylpyrene; ER-ITC, erythrosin 5′-isothiocyanate; GPIIb/GPIIIa, heterodimer of glycoproteins GPIIb and GPIIIa.

0006-2960/92/0431-7580$03.00/0

fraction of bent molecules observed in the electron micrographs. This viewpoint, although at variance with our findings (Acuña et al., 1987a,b) on the lack of flexibility of the protein core, has been adopted by some authors (Larsson et al., 1987; Apap-Bologna et al., 1989), who proposed that large conformational flexibility in the protein can be brought about by decreasing or increasing (respectively) the Ca^{2+} concentration in the solution.

In the present work, we investigate the hydrodynamic form and dimensions of human fibrinogen by measuring the individual rotational correlation times of the protein in solution. Since in the case of a large, elongated molecule, such as fibrinogen, these time constants appear in the microsecond time range, we resort to the rotational depolarization of electronic transitions associated with the triplet state of bonded optical probes (Naqvi et al., 1973; Cherry et al., 1976; Pochon et al., 1978; Garland & Moore, 1979). The interpretation of the microsecond rotational relaxation measurements depends on whether or not the protein is rigid. Therefore, considering the two (conflicting) recent claims on protein flexibility as a function of Ca^{2+} concentration, we also present here additional fluorescence anisotropy data, as a function of the concentration of Ca^{2+} and with increased time resolution, that confirm our previous model (Acuña et al., 1897a,b) of the molecule as an overall rigid structure, in the sense mentioned above.

MATERIALS AND METHODS

Protein Preparation. Human fibrinogen (Kabi, Stockholm), after extensive dialysis, was derivatized to obtain two different conjugates, to be used in the fluorescence depolarization and triplet experiments. The fluorescent conjugate MePy-FIB contained 1-methylpyrene, that was covalently bound by reacting 1-pyrenealdehyde (Aldrich, recrystallized) with the free amino groups of fibrinogen to form a Schiff base; the base was reduced with $NaBH_4$. This procedure, described in detail elsewhere (Acuña et al., 1987a), provides homogeneously labeled fibrinogen with a dye:protein molar ratio of ≈0.3. The buffer composition for the fluorescence measurements was 50 mM Tris-HCl, 150 mM NaCl, 1.5 mM $CaCl_2$, and 3 mM Na_3N, pH 7.4. Erythrosin 5′-isothiocyanate (ER-ITC) was used as the triplet labeling reagent by adding the dye in a 5:1 molar ratio to a fibrinogen solution (10 mg/mL) in 20 mM sodium phosphate buffer, with 150 mM NaCl and 1 mM EDTA, pH 8. The mixture, kept at 20 °C for 2 h, was filtered through Sephadex G-50 and fractionated in a Sephacryl S400 column. The purified conjugate was finally diluted down to 1 mg/mL in 20 mM sodium phosphate, 150 mM NaCl, 1 mM EDTA, and 3 mM Na_3N, pH 7.4. The random distribution of the dye in fibrinogen was determined by controlled reduction and enzymatic digestion of the protein, followed by HPLC and gel electrophoresis analysis, as with the fluorescent derivatives (Acuña et al., 1987a). Functional tests (clottability) and ultracentrifugation analysis (to check the absence of aggregates) were carried out along with the labeling process and spectroscopic measurements. The absorption spectrum of the erythrosinylfibrinogen derivative was very similar to that of the free dye, presenting a red-shift of the first absorption maximum of ≈10 nm. A value of the absorption coefficient of $\approx 10^5$ M^{-1} cm^{-1} at λ_{max} = 538 nm (Garland & Moore, 1979) was used to estimate the dye:protein molar ratio, usually in the 2–3 range. The samples were deoxygenated with the enzymatic reaction of glucose oxidase/catalase (Horie & Vanderkooi, 1981). Triplet lifetimes became maximal about 15 min after addition of the enzymes.

Polarized Laser Flash Photolysis. The time-resolved triplet dichroism was measured in a laser flash photolysis spectrometer, where the excitation pulses (15 ns) were generated with a Molectron MY34 Nd:YAG laser, Q-switched and frequency-doubled (532 nm), operating at 10 Hz. The pulses were repolarized (vertically) with a Glan–Thompson calcite crystal, attenuated (2–3 mJ), and focused on the sample cuvette as to cover the area analyzed by the probe beam (10 × 1 mm). This probe beam, from a chopped 100-W tungsten–iodine lamp at 90° to the excitation beam, was focused on the slit of a 0.25-m Jarrel–Ash monochromator. Two additional polarizers were inserted between the sample and monochromator; the first one was used to analyze the components of the transmitted light parallel ($I_\parallel$) and perpendicular ($I_\perp$) to the electric vector of the excitation pulse. The second one was adjusted (≈45°) to give equal signals in the detection photomultiplier (Hamamatsu R928) for vertical and horizontal orientations of the analyzer, when the sample was excited with horizontally polarized light. The orientation of this compensating polarizer had to be determined for the actual experimental conditions (gain and time range) of the digitizer (Tektronix 7912AD), to correct for the static (Eads et al., 1984) and time-dependent (Restall et al., 1984) polarization artifacts. The usual procedure of determining a correction factor to be used in later analysis did not give in our hands enough accuracy for transmission changes in the 1% range. The time resolution of the spectrometer was 40 ns, with a dead time of 100–200 ns produced by the recovery time of the photodetector.

Fluorescence Depolarization. The decay of the polarized fluorescence of MePy-FIB was recorded in an improved version of a time-correlated single-photon counting spectrometer (Acuña et al., 1987a), using a nanosecond flash lamp (Edinburgh Instruments EI 199) filled with N_2 or H_2. Polaroid HNP′B sheets were used in the excitation and emission channels.

Data Analysis: (*A*) *Absorption.* The triplet anisotropy (dichroism) function is given by

$$R(t) = [\Delta A_\parallel(t) - \Delta A_\perp(t)]/[\Delta A_\parallel(t) + 2\Delta A_\perp(t)] \quad (1)$$

where the absorbance changes, ΔA, are obtained from

$$\Delta A_\parallel(t) = \log [I_0/I_\parallel(t)]; \; \Delta A_\perp(t) = \log [I_0/I_\perp(t)] \quad (2)$$

The transmitted intensity $I_t(t)$ was greater than I_0 when the probe beam was at 538 nm (ground-state depletion) and was less than I_0 when the probe beam recorded the T–T absorption (580–620 nm) of the erythrosin chromophore. The $R(t)$ decay curves were analyzed by a nonlinear least-squares routine in terms of mono- and multiexponential models:

$$R(t) = \sum^{N} \alpha_i \exp(-t/\phi_i) \; (N = 1, 2, 3) \quad (3)$$

The initial slope of the decay curve is given by

$$[dR(t)/dt]_{t=0} = -\sum(\alpha_i/\phi_i) = -1/\phi_0 \quad (4)$$

where ϕ_0 is the average initial correlation time.

The physical significance of the variables α_i and ϕ_i depends on the particular rotational model considered and is discussed below. The quality of the fitting was determined from the values of the residual variance RV (sum of the unweighted squared residuals) and the randomness of the residuals, defined as the differences between the best-fitting function and the data. The relative uniform distribution of the residuals gives support to the equal-weights analysis. Since the anisotropy decay times of fibrinogen in solution span a large time domain,

Table I: Decay Parameters of the Fluoresence Intensity and Anisotropy of Methylpyrenylfibrinogen (MePy-FIB) as a Function of [Ca^{2+}] at 20 °C[a]

[Ca^{2+}]	a_1	τ_1	a_2	τ_2	a_3	τ_3	a_4	τ_4	α_1	ϕ_1	α_2	ϕ_2
$\sim 10^{-8}$ M[b]	0.49 (0.02)	1 (0.2)	0.17 (0.01)	7 (1)	0.17 (0.01)	25 (2)	0.17 (0.01)	100 (2)	0.30 (0.01)	10 (5)	0.70 (0.02)	800 (100)
1.5 mM[c]	0.50 (0.02)	1 (0.2)	0.22 (0.02)	7 (1)	0.16 (0.01)	25 (2)	0.12 (0.01)	100 (2)	0.30 (0.01)	20 (5)	0.70 (0.02)	800 (100)

[a] The decay of the fluorescence intensity was fitted to a four-exponential function, $i_F = \sum a_i \tau_i$ (τ = lifetime in nanoseconds); the anisotropy was analyzed with the expression $r(t) = r(0)[\alpha_1 \exp(-t/\phi_1) + \alpha_2 \exp(-t/\phi_2)]$ where ϕ = correlation time in nanoseconds and $\sum \alpha_i = 1$; $r(0) = 0.14$, independent of [Ca^{2+}]. Numbers in parentheses indicate sample-to-sample variation. [b] 20 mM sodium phosphate, 150 mM NaCl, 1 mM EDTA, and 3 mM Na_3N, pH 7.4. [c] 50 mM Tris-HCl, 150 mM NaCl, 1.5 mM $CaCl_2$, and 3 mM Na_3N, pH 7.4.

from ≈300 ns to ≈3–4 μs, several (50–70) decay sets [$I_\parallel(t)$, $I_\perp(t)$] were recorded for each time range at different values of the time sweep of the digitizer, from 4 to 40 ns/point (512 points). Finally, the averaged traces were added to generate the data files for analysis. In this way, there is a higher density of experimental values in the initial part of the decay, and apparently, this compensates for the higher noise level of the fastest time ranges. A further check for systematic errors was carried out by comparing the decay parameters of the sum function, $S(t) = \Delta A_\parallel(t) + 2\Delta A_\perp(t)$, with those of the intensity recorded at the magic angle, $I_{54}(t)$.

(B) Fluorescence. The fluorescence anisotropy decay function, $r(t)$, was determined by fitting the emission intensities $I_\parallel(t)$ and $I_\perp(t)$ simultaneously by a nonlinear least-squares global analysis method, developed from published sources (Knutson et al., 1983; Cross & Fleming, 1984; Löfroth, 1985) as detailed elsewhere (Mateo et al., 1991). The "reference" technique was used in the analysis of the fluorescence lifetimes, as described elsewhere (Mateo et al., 1991).

Transmission Electron Microscopy. Samples of fibrinogen in 50 mM Tris-HCl, 0.1 mM $CaCl_2$ (pH 7.4) were diluted to 20 μg/mL with a 2:1 (v/v) buffer/glycerol mixture and sprayed onto 1 cm^2 pieces of freshly cleaved mica. After 30 min of drying at 10^{-6} torr, the samples were rotary-shadowed with platinum/carbon film at 5° and backed with a 15-nm-thick carbon layer. EM observations were carried out in a Siemens Elmiskop 1A at 80 kV.

RESULTS AND DISCUSSION

Fluorescence Anisotropy Decay of Methylpyrenylfibrinogen. The fluorescence intensity decay of the protein labeled with 1-methylpyrene in a 1.5 mM Ca^{2+} solution, close to physiological conditions, was fitted to a four-exponential function (Table I), giving an average lifetime ($\sum a_i\tau_i^2/\sum a_i\tau_i$) of 80 ns. This decay was independent of the calcium concentration (10^{-3}–10^{-8} M). The time-resolved fluorescence anisotropy (Figure 1) was analyzed with a biexponential function containing a fast rotational relaxation time of 20 ns and a slow one of ≈800 ns (Table I). The low value of the initial anisotropy, $r(0) = 0.14$, compared with that measured with the methylpyrene chromophore in rigid matrices (0.21) is due to an additional subnanosecond motion (<300 ps) that could not be resolved accurately. The decay of the fluorescence anisotropy of these fibrinogen samples is virtually the same as that observed in the absence of calcium (≈10^{-8} M), as shown in Table I. The only significant difference is the retardation of the fast relaxation time, from ≈10 to 20 ns, in the presence of Ca^{2+}. Moreover, the anisotropy decay parameters of the labeled fibrinogen samples in the absence of Ca^{2+} iterated here (Table I) reproduced those of our previous work (Acuña et al., 1987a,b), obtained with different detection photomultiplier, timing electronics, and numerical analysis techniques.

The fast depolarization observed in the 0.3–20-ns time range might arise from the restricted motion of small fragments of

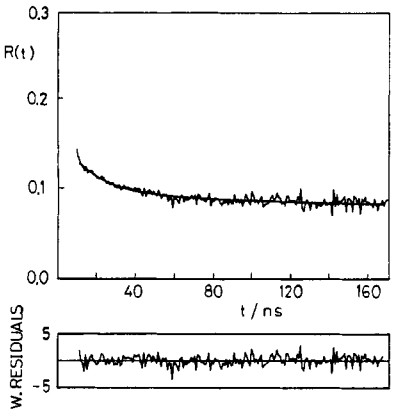

FIGURE 1: Decay of the fluorescence anisotropy of 1-methylpyrenylfibrinogen in the presence of Ca^{2+} at 20 °C. The buffer composition was 50 mM Tris-HCl, 150 mM NaCl, 1.5 mM $CaCl_2$, and 3 mM Na_3N. The fitting parameters of the overlayed anisotropy function are $\phi_1 = 20$ ns, $\alpha_1 = 0.27$, $\phi_2 = 800$ ns, $\alpha_2 = 0.73$, $r(0) = 0.14$, and reduced $\chi^2 = 1.14$.

polypeptide chains. Since no additional depolarizing motions are observed in experiments covering up to almost 1 μs, the protein core appears rigid in this time interval (15–1000 ns), independently of the Ca^{2+} concentration. This confirms our previous data and excludes the possibility of large calcium-dependent conformational changes. The effect of calcium on the conformation of fibrinogen in solution was also investigated by Van der Drift et al. (1983), from measurements of viscosity and sedimentation coefficients. In that work, it was concluded that the binding of Ca^{2+} up to 20 mM concentration has no obvious effect on the protein conformation.

Decay of the Triplet Anisotropy in Erythrosinylfibrinogen. The ground-state and triplet–triplet absorption spectra of the erythrosin chromophore covalently bound to fibrinogen are shown in Figure 2. The decay of the triplet state of ER-FIB in the degassed buffer is best described by a two-exponential function with lifetimes (amplitudes) of 2.6 (0.36) and 22 (0.64) μs (Figure 2) when monitored both from the transient absorption at 580 nm and from the recovery of the ground-state depletion at 538 nm. This is much faster than the decay of the free dye in the same conditions (38 and 103 μs), indicating that the excited triplet population is being quenched by the protein. Since the dichroism and S/N ratio of the ground-state depletion signal were much higher than those of the T–T absorption, the rotational relaxation of ER-FIB was measured by monitoring the recovery of the polarized transmission at 538 nm. The two time-resolved polarized components of the transmitted light are shown in Figure 3 for the extreme values of the time ranges studied here (4 and 40 ns/point, respectively). The first 200 ns contains the fast decay associated with the recovery time of the detection setup and, therefore, was not included in the analysis. The initial dichroism, $r_{200ns} \approx 0.2$, is close to that observed (Garland & Moore, 1979) for the free dye in solid matrices (0.25–0.28), decaying to a zero value after 10–12 μs (Figure 4). The

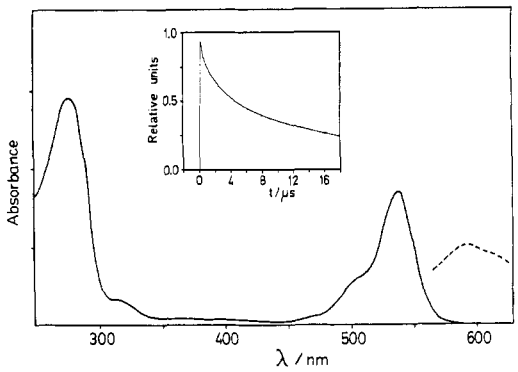

FIGURE 2: Ground-state (—) and T–T absorption (- - -) spectra of a 1 mg/mL solution of erythrosinylfibrinogen (dye:protein molar ratio of 3) in 20 mM sodium phosphate, 150 mM NaCl, 1 mM EDTA, and 3 mM Na_3N, pH 7.4. The solution contained the enzymatic deoxygenating mixture. *Inset*: Transient transmittance change at the wavelength of the T–T absorption (580 nm) in the same sample. The fitting parameters of the decay were $\tau_1 = 2.6$ μs, $a_1 = 0.36$, $\tau_2 = 22$ μs, and $a_2 = 0.64$.

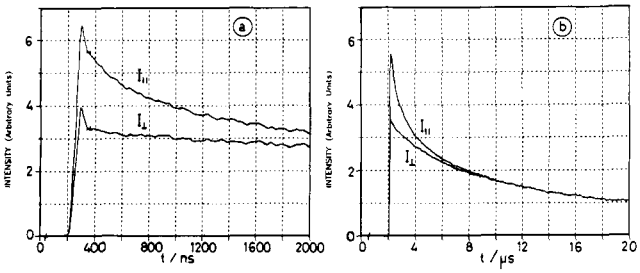

FIGURE 3: Time-resolved dichroism of the triplet state of erythrosinylfibrinogen at 20 °C. The changes in the polarized transmitted intensity ($I_\parallel$, $I_\perp$) were recorded by monitoring the ground-state depletion signal at 538 nm, with 2-mJ pulses of laser excitation at 532 nm. (a) Decay recorded at the fastest time resolution showing the recovery time of the photodetector. (b) Signals recorded in the slowest time range showing the decay of laser-induced anisotropy by overall rotational diffusion of the protein.

experimental dichroism traces were fitted to eq 3 as described above using the following models.

Model I is a pure numerical approximation where all parameters in eq 3 are considered variables. The three-exponential function ($N = 3$) gives some improvement in the goodness-of-fit parameters compared with the biexponential ($N = 2$) (Figure 4 and Table II) and much better than the single-exponential decay, ruling out a rigid spherical shape for the protein. The introduction of additional exponential terms ($N = 4, 5$) did not result in a statistically significant improvement. Therefore, the decay of the dichroism of ER-FIB at 20 °C is completely described within this approximation by a very fast relaxation time (330 ns) and two additional relaxation times in the microsecond range (1.1 and 3.55 μs).

Model II (*A and B*). The images of fibrinogen observed by EM and AFM suggest that the shape of the protein in solution might be approached by a particle with cylindrical symmetry, characterized by two rotational diffusion coefficients ($D_\parallel$ and $D_\perp$). Moreover, taking account of the randomness of the labeling, the decay of the dichroism would be given by (Chuang & Eisenthal, 1972; Ehrenberg & Rigler, 1972):

$$r(t) = r_0[\alpha_1 \exp(-t/\phi_1) + \alpha_2 \exp(-t/\phi_2) + \alpha_3 \exp(-t/\phi_3)] \quad (5)$$

where $\phi_1 = (2D_\perp + 4D_\parallel)^{-1}$, $\phi_2 = (5D_\perp + D_\parallel)^{-1}$, $\phi_3 = (6D_\perp)^{-1}$,

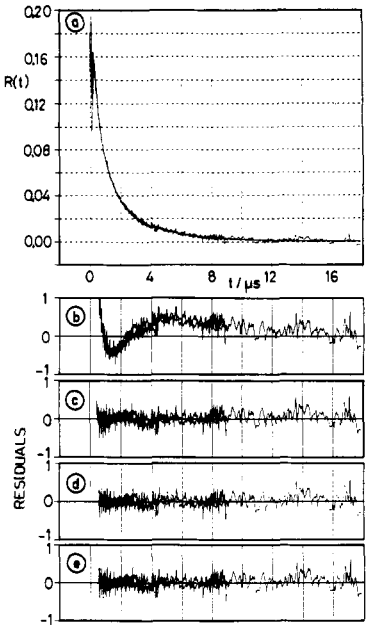

FIGURE 4: (a) Decay of the anisotropy of erythrosinylfibrinogen at 20 °C in solution measured from the laser-induced ground-state depletion. (b) The residuals of the fit to a one-exponential, (c) two-exponential, and (d) three-exponential function with all parameters free (model I). (e) Residuals of the fit to the exponential function of model IIB. The fitting parameters are listed in Table II.

and

$$\alpha_1 = \alpha_2 = 2\alpha_3 = 2/5 \quad (6)$$

The average correlation time for the initial decay can be computed (Wahl, 1983) as

$$\phi_0 = (4D_\perp + 2D_\parallel)^{-1} \quad (7)$$

By equating $R(t) = r(t)/r_0$, the expression in eq 5 becomes

$$R(t) = \alpha_1 \exp(-t/\phi_1) + \alpha_2 \exp(-t/\phi_2) + \alpha_3 \exp(-t/\phi_3) \quad (8)$$

Equation 8 can be used to analyze the decay of the experimental dichroism by taking the three correlation times as adjustable quantities (model IIA), or, alternatively, the ϕ_i values can be expressed as functions of the rotational diffusion coefficients ($D_\parallel$ and $D_\perp$), so the number of independent variables is decreased by 1 (model IIB). In both cases, the values of the preexponential factors are given by eq 6. The residuals distribution of the fit of the experimental decay of the ER-FIB triplet dichroism to model IIB is shown in Figure 4e, and Table II contains the fitting parameters for models IIA and IIB. The fitting data (Table II) indicate that the rotational correlation times are similar to those obtained when all six parameters in eq 8 are left free, as in model I. The rotational diffusion coefficients of human fibrinogen computed from model IIB and averaged over all the samples investigated here are shown in Table III. If one makes the additional assumption that the hydrodynamics of the protein in solution may be modeled by that of an ellipsoid of revolution (semi-major axis a, semiminor axis b, axial ratio $p = a/b$) or of a cylinder ($p = L/d$), the oblate and disk shapes, which imply that $D_\perp > D_\parallel$, are ruled out.

The average initial rotational correlation time that should be observed in a nanosecond fluorescence depolarization experiment can be computed from the triplet data (Table III, eq 7) as 0.7 ± 0.1 μs. The *experimental* value of ϕ_0 can be estimated from the slope of the slowest part of the decay of the fluorescence anisotropy in the 400-ns time range. Thus, ϕ_0 goes from 1.1 ± 0.1 μs (Acuña et al., 1987b) to 0.8 ± 0.1

Table II: Analysis of the Transient Anisotropy Decay of Erythrosinylfibrinogen Monitored at 538 nm[a]

model[b]	N	α_1	ϕ_1	α_2	ϕ_2	α_3	ϕ_3	RV[c]
I	1	0.2	1.39					26
	2	0.14	0.62	0.06	2.77			2.5
	3	0.09	0.33	0.072	1.10	0.038	3.55	2.0
IIA	3	0.4	0.34	0.4	1.12	0.2	3.56	2.1
IIB	3	0.4	0.39	0.4	1.14	0.2	3.1	2.2
⟨IIB⟩	3	0.4	0.38 (0.05)	0.4	1.1 (0.1)	0.2	3.3 (0.6)	

[a] The data collected at 4, 10, 20, and 40 ns/point were fitted simultaneously to the expression $R(t) = \sum^N \alpha_i \exp(-t/\phi_i)$ for $N = 1, 2, 3$, with the indicated constraints (ϕ = correlation time in microseconds). 20 mM sodium phosphate, 150 mM NaCl, 1 mM EDTA, and 3 mM Na_3N, pH 7.4, 20 °C. [b] Model I, all parameters free; IIA, $\alpha_1 = \alpha_2 = 2\alpha_3 = 2/5$, ϕ_i free; IIB, $\alpha_1 = \alpha_2 = 2\alpha_3 = 2/5$, $\phi_1 = (2D_\perp + 4D_\parallel)^{-1}$, $\phi_2 = (5D_\perp + D_\parallel)^{-1}$, $\phi_3 = (6D_\perp)^{-1}$; ⟨IIB⟩, mean values of three independent preparations. Numbers in parentheses indicate sample-to-sample variation. [c] Normalized residual variance defined as the sum of unweighted squared residuals.

Table III: Dimensions of Hydrodynamic Models and Diffusive Properties of Human Fibrinogen in Aqueous Solution at 20 °C

	symbol (units)	this work	lit values (ref)[a]
prolate ellipsoid	$2a \times 2b$ (nm)	$(54 \pm 6) \times (7.2 \pm 0.5)$	b
cylinder	$L \times d$ (nm)	48 × 6.4	48 × 7.6 (*c*), 45 × 9 (*d*)
hydrated volume	V_h (nm³)	1500 ± 200	2200 (*c*), 2860 (*d*)
dry volume	V (nm³)		410 (*d*)
translational diffusion	D_t (10^{-11} m² s⁻¹)	2.16[i]	2.07 (*d*)
rotational diffusion	$D_\parallel$ (10^5 s⁻¹)	6.2 ± 0.7	16 (*e*)
	$D_\perp$ (10^4 s⁻¹)	5 ± 1	5 ± 1.5 (*f*), 3–9.7 (*g*)
initial slope[j]	ϕ_0 (ns)	0.7[i]	0.8–1.1 (this work, *h*)

[a] Only recent measurements are included; for a comprehensive revision of previous data, see Doolittle (1973). [b] Literature values (length) range from 25 to 100 nm (see text). [c] López et al. (1984). [d] Van der Drift et al. (1983). [e] Serralach et al. (1979). [f] Wiltzius & Hofman (1980). [g] Larsson et al. (1987). [h] Acuña et al. (1987 a,b). [i] Calculated by standard expressions for the ellipsoid tabulated here. [j] Average rotational correlation time in a fluorescence anisotropy decay experiment.

μs in the present work, which agrees quite well with the value predicted from the triplet anisotropy measurements, considering that the 400-ns interval of the fluorescence anisotropy decay contains a sizeable contribution from the ϕ_2 time constant.

Hydrodynamic Dimensions of Fibrinogen. The hydrodynamic approximation, together with the reasonable assumption that the motion of water relative to the surface of a macromolecule as large as fibrinogen can be described by the *stick* boundary condition, can be used to estimate the shape and dimensions of the hypothetical rigid particle (if any) which would have the rotational correlation times determined here. However, as the rotational diffusion coefficients—and therefore the rotational correlation times—depend on the axial ratio and the volume of the particle (Perrin, 1934), at least two independent measurements are required to get the dimensions of the diffusing body. Here, we followed one of the former suggestions of Scheraga and Mandelkern (1953) and combined our measurements of the protein rotational coefficients (Table III) with the experimental *intrinsic viscosity*, $[\eta]$, which is defined usually as

$$[\eta] = \upsilon N_A V_h / M \tag{9}$$

where υ is the Einstein–Simha factor (Einstein, 1911; Simha, 1940; Jeffrey, 1923), N_A the Avogadro constant, V_h the volume of the hydrated particle, and M the molar mass. The intrinsic viscosity of fibrinogen has been determined several times, giving values clustered around 25 ± 1 cm³ g⁻¹. Hence, from eq 9 and the Perrin (1934) expressions for the rotational coefficients, the relations are immediately obtained:

$$D_\parallel = \Omega_\parallel (kTN_A / 6\eta_w [\eta] M) \tag{10a}$$

$$D_\perp = \Omega_\perp (kTN_A / 6\eta_w [\eta] M) \tag{10b}$$

$$\Omega_i = \upsilon / F_i$$

where η_w is the solution viscosity and F_i are the rotational friction factors relative to that of the equivalent spherical particle. Since both υ and F_i depend only on the axial ratio, from the experimental values of D_t and $[\eta]$ one might obtain the axial ratio and volume of the protein. This procedure has two important disadvantages. First, as the value of $\Omega_\perp$ is not very sensitive to the axial ratio in the range of $p > 4$, small experimental errors in $D_\perp$ and $[\eta]$ values give rise to a large uncertainty in the estimated shape of the particle. Second, the accuracy of the diffusion coefficients is limited by the ill-defined nature of the multiexponential analysis used to obtain those values. Therefore, it seemed physically more correct to apply the above expressions using an inverse technique in a stepwise procedure. Thus, the rotational diffusion coefficients and correlation times for ellipsoids with axial ratios in the range of 1–20 were computed from eq 10 and 5, respectively, using the experimental values of the intrinsic viscosity of the protein. Graphs such as those of Figure 5 were obtained, showing the expected correlation times as a function of the axial ratio for prolate and oblate particles characterized by the intrinsic viscosity of fibrinogen (the curves corresponding to the complete experimental range of the intrinsic viscosity values were omitted for clarity). The data of Figure 5 show that the oblate geometry is not consistent simultaneously with the observed correlation times (Table II) and intrinsic viscosity. On the other hand, a prolate ellipsoid with axial ratio of ≈7.5 would present rotational correlation times compatible both with the experimental values determined here and with the range of intrinsic viscosity values recorded in the literative (vida supra). The dimensions ($2a \times 2b$) of this particle would be $(54 \pm 6) \times (7.2 \pm 0.5)$ nm, with a (hydrated) volume of 1500 ± 200 nm³. This model is drawn in Figure 6A, overlaying the contour of the fibrinogen globular domains joined by rodlike connectors first observed in the electromicrographs (Hall & Slater, 1959) of the dry protein (Figure 6B) and later in the AFM images of the molecule in solution (Drake et al., 1989). It is interesting that both the shape and dimensions of this model are remarkably close to the estimates derived from the nanosecond fluorescence depolarization measurements (Acuña et al., 1987a,b).

Alternatively, the rotational diffusion constants may be interpreted by means of the semiempirical expressions of some of the transport properties of *cylindrical* particles now available (López et al., 1984; Tirado & García de la Torre, 1979, 1980). Although no practical complete theory exists for computing the $[\eta]$ of cylinders, it has been found (J. García de la Torre,

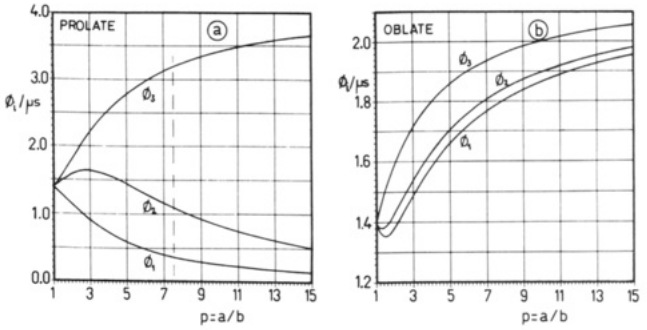

FIGURE 5: Rotational correlation times (water, 20 °C) of fibrinogen modeled as a rigid particle with cylindrical symmetry. These specific values of ϕ_i were obtained as a function of the axial ratio p for prolate and oblate geometry, taking a value of 25 cm^3/g for the intrinsic viscosity of the protein.

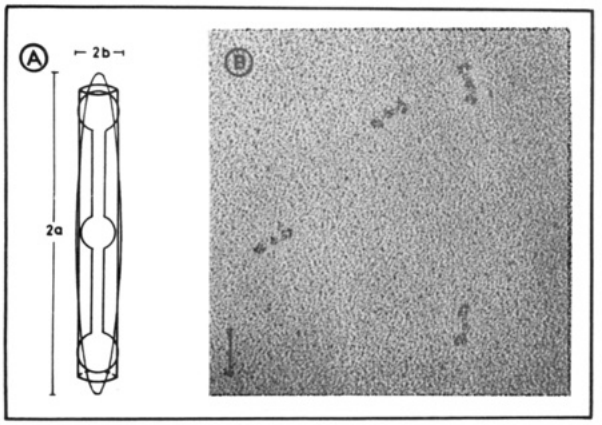

FIGURE 6: (A) Scaled overlay of the EM image of fibrinogen from Hall and Slayter (1959) and the ellipsoidal and rod hydrodynamic models derived from triplet rotational diffusion data. (B) Transmission EM images of the fibrinogen samples used in this work. Magnification 120000×; bar = 50 nm.

personal communication) that, in the range of axial ratios of 5–10, a cylindric particle would have virtually the same intrinsic viscosity as that of the *equivalent* prolate ellipsoid (i.e., that with the same volume and rotational diffusion coefficients as those of the cylinder). Accordingly, a cylindric particle with the values of $[\eta]$, $D_\parallel$, and $D_\perp$ of fibrinogen (Table III) would have dimensions of ≈48 × 6.4 nm (Figure 6A), that are to be compared with those proposed before (47 × 7.6 nm) on the basis of diffusion data available a that time (López et al., 1984).

Since the *dry* volume of the protein, computed from the molecular weight and partial specific volume (0.724 cm^3 g^{-1}; Van der Drift et al., 1983), is 410 nm^3, both models of the fibrinogen conformation in solution—ellipsoidal and cylindric—would be hydrated with up to ≈2 g of H_2O/g of protein. Finally, in Table III the diffusional properties of the protein estimated using the dimensions of the model proposed here are compared with the corresponding experimental values determined by alternative techniques. The tabulated data show that the spectroscopic methods described in this work provide extensive information of the transport properties of fibrinogen in solution.

In conclusion, by combining fluorescence and triplet polarization spectral methods, the rotational motions of human fibrinogen in near-physiological solution could be recorded over a time range of 3 orders of magnitude, from a few nanoseconds to tens of microseconds. The nanosecond measurements reported here as a function of Ca^{2+} concentration indicate the absence (in this time domain) of large conformational changes induced by this ion in the relatively rigid core of the protein, in divergence with previous (contradicting) reports. The microsecond triplet techniques provided information on the overall conformation of fibrinogen in solution, showing that the protein can be modeled by rigid ellipsoids or cylinders with dimensions that match those of the EM and AFM images.

These observations bear some functional consequences. The rigid representation of fibrinogen in solution suits the requirements of the classical half-staggered double-stranded model for fibrin polymerization (Ferry, 1952; Stryer et al., 1963; Rao et al., 1991), as we pointed out before (Acuña et al., 1987b). It is also consistent with what it is known so far on the fibrinogen function in platelet agreggation, where its lack of flexibility would prevent the cross-linking of receptors (the GPIIb/GPIIIa complex) within the surface of the same platelet while it favors the interaction with neighbor cells. On the other hand, it is difficult to conciliate a stiff fibrinogen with the recently proposed interlocked single-stranded mechanism (Hunziker et al., 1990) in which the fibrin monomers had to be very flexible and with a high radial symmetry of polymerization sites.

ACKNOWLEDGMENT

We acknowledge several helpful discussions with Dr. García de la Torre on the hydrodynamics of cylindric objects. We also thank Dr. F. Amat, Dr. G. Rivas, and M. del Mar López for assistance in sample preparation and Dr. J. A. Aznarez and J. M. Sánchez for help with the EM pictures.

REFERENCES

Acuña, A. U., González-Rodríguez, J., Lillo, M. P., & Razi Naqvi, K. (1987a) *Biophys. Chem. 26*, 63.
Acuña, A. U., González-Rodríguez, J., Lillo, M. P., & Razi Naqvi, K. (1987b) *Biophys. Chem. 26*, 51.
Apap-Bologna, A., Webster, A., Raitt, F., & Kemp, G. (1989) *Biochim. Biophys. Acta 995*, 70.
Bachmann, L., Schmitt-Fumian, W. W., Hammel, P., & Lederer, K. (1975) *Makromol. Chem. 176*, 2603.
Beijbom, L., Larsson, U., Kavéns, U., & Hebert, H. (1988) *J. Ultrastruct. Mol. Struct. Res. 98*, 312.
Cherry, R. J., Cogoli, A., Oppliger, M., Schneider, G., & Semenza, G. (1976) *Biochemistry 15*, 3653.
Chuang, T. J., & Eisenthal, K. B. (1972) *J. Chem. Phys. 57*, 5094.
Cross, A. J., & Fleming, G. R. (1984) *Biophys. J. 46*, 45.
Doolittle, R. F. (1973) *Adv. Protein Chem. 27*, 1.
Drake, B., Prater, C. B., Weisenhorn, A. L., Gould, S. A. C., Albretch, T. R., Quate, C. F., Canell, D. S., Hansma, H. G., & Hansma, P. K. (1989) *Science 243*, 1586.
Eads, T. M., Thomas, D. D., & Austin, R. H. (1984) *J. Mol. Biol. 179*, 55.
Ehrenberg, M., & Rigler, R. (1972) *Chem. Phys. Lett. 14*, 539.
Einstein, A. (1911) *Ann. Phys. (Leipzig) 34*, 591.
Erickson, P. H., & Fowler, W. E. (1983) *Ann. N.Y. Acad. Sci. 408*, 146.
Ferry, J. D. (1952) *Proc. Natl. Acad. Sci. U.S.A. 38*, 566.
Fowler, W. E., & Erickson, P. H. (1979) *J. Mol. Biol. 134*, 241.
Garland, P. B., & Moore, C. H. (1979) *Biochem. J. 183*, 561.
Hall, C. E., & Slayter, H. S. (1959) *J. Biophys. Biochem. Cytol. 5*, 11.
Haverkate, F., Henschen, A., Nieuwenhuizen, W., & Straub, P. W., Eds. (1983) in *Fibrinogen. Structure, Functional Aspects, Metabolism*, Walter de Gruyter, Berlin.
Horie, T., & Vanderkooi, J. M. (1981) *Biochim. Biophys. Acta 670*, 294.
Hunziker, E. B., Straub, P. W., & Haeberli, A. (1990) *J. Biol. Chem. 265*, 7455.
Jeffrey, G. B. (1923) *Proc. R. Soc. London, A 102*, 163.

Kieffer, N., & Phillips, D. R. (1990) *Annu. Rev. Cell Biol. 6*, 329.
Knutson, J. R., Beechem, J., & Brand, L. (1983) *Chem. Phys. Lett. 102*, 501.
Larsson, U., Blombäck, B., & Rigler, R. (1987) *Biochim. Biophys. Acta 917*, 172.
Lederer, K. (1975) *Makromol. Chem. 176*, 2653.
Lederer, K., & Hammel, R. (1975) *Makromol. Chem. 176*, 2619.
Löfroth, J. E. (1985) *Eur. J. Biophys. 13*, 45.
López, M. C., Rodes, V., & García de la Torre, J. (1984) *Int. J. Biol. Macromol. 6*, 261.
Mateo, C. R., Lillo, M. P., González-Rodríguez, J. G., & Acuña, A. U. (1991) *Eur. Biophys. J. 20*, 41.
Mueller, M., & Burchard, W. (1978) *Biochim. Biophys. Acta 537*, 208.
Naqvi, R. K., González-Rodríguez, J., Cherry, R. J., & Champman, D. (1973) *Nature (London), New Biol. 245*, 249.
Perrin, F. (1934) *J. Phys. Rad. 5(7)*, 497.
Pochon, F., Amand, B., Lavalette, D., & Bieth, J. (1978) *J. Biol. Chem. 253*, 7496.
Rao, S. P. S., Poojary, M. D., Elliot, B. W., Melanson, L. A., Oriel, B., & Cohen, C. (1991) *J. Mol. Biol. 222*, 98.
Restall, C. J., Dale, R. E., Murray, E. K., Gilbert, C. W., & Champman, D. (1984) *Biochemistry 23*, 6765.
Rivas, G., Aznárez, J. A., Usobiaga, P., Saíz, J. L., & González-Rodríguez, J. (1991) *Eur. Biophys. J. 19*, 335.
Scheraga, H., & Mandelkern, L. (1953) *J. Am. Chem. Soc. 75*, 179.
Serrallach, E. N., Hofmann, V. E., Zulauf, M., Binkert, T., Hofmann, R., Kanzig, W., Straub, P. W., & Schwyzer, R. (1979) *Thromb. Haemostasis 41*, 648.
Simha, R. (1940) *J. Phys. Chem. 44*, 25.
Stryer, L., Cohen, C., & Laugridge, R. (1963) *Nature 197*, 793.
Tirado, M. M., & García de la Torre, J. (1979) *J. Chem. Phys. 71*, 2581.
Tirado, M. M., & García de la Torre, J. (1980) *J. Chem. Phys. 73*, 1986.
Van der Drift, A. C. M., Poppema, A., Havekarte, F., & Nieuwenhuizen, W. (1983) in *Fibrinogen. Structure, Functional Aspects, Metabolism* (Haverkate, F., Henschen, A., Nieuwehuizen, W., & Straw, P. W., Eds.) p 3, Walter de Gruyter, Berlin.
Whal, Ph. (1983) *NATO ASI Ser., Ser. A 69*, 497.
Wigren, R., Elwing, H., Erladsson, R., Welin, S., & Lundström, I. (1991) *FEBS Lett. 280*, 225.
Wiltzius, P., & Hofmann, V. (1980) *Thromb. Res. 19*, 793.